Original Article

^{18}F-fluorodeoxyglucose positron emission tomography-computed tomography for predicting pathological complete response to neoadjuvant chemotherapeutic in breast cancer patients

Chengchun Ge, Lukai Shi, Zhonghua Tan

Department of Nuclear Medicine, Affiliated Hospital of Nantong University, Nantong, China

Contributions: (I) Conception and design: C Ge; (II) Administrative support: None; (III) Provision of study materials or patients: Z Tan; (IV) Collection and assembly of data: L Shi; (V) Data analysis and interpretation: C Ge; (VI) Manuscript writing: All authors; (VII) Final approval of manuscript: All authors.

Correspondence to: Zhonghua Tan, PhD. Department of Nuclear Medicine, Affiliated Hospital of Nantong University, 20 Xisi Road, Nantong 226000, China. Email: zhhtan@126.com.

Background: Accurately predicting pathological complete response (pCR) to neoadjuvant chemotherapy (NACT) in breast cancer remains a clinical challenge. Current imaging-based models are limited in their ability to integrate key metabolic parameters to enhance prediction accuracy. This study aimed to develop and validate a nomogram using ^{18}F-fluorodeoxyglucose (FDG) positron emission tomography/computed tomography (PET/CT) parameters, including maximum standardized uptake value (SUV_{max}), metabolic tumor volume (MTV), and total lesion glycolysis (TLG), to improve pCR prediction. These parameters, representing both tumor metabolic burden and activity, were hypothesized to collectively provide a robust means of predicting pCR.

Methods: This retrospective cohort study enrolled 95 breast cancer (BC) patients who underwent ^{18}F-FDG PET/CT before and after NACT. Patients were categorized into pCR (n=46) and non-pCR (n=49) groups based on postoperative pathological outcomes. Clinical and pathological characteristics, as well as changes in SUV_{max}, MTV, and TLG, were compared between the two cohorts. Logistic regression identified independent predictors of non-pCR. The dataset was then randomly divided into training (n=66) and validation (n=29) cohorts for nomogram construction and validation. The model's performance was evaluated using the area under the receiver operating characteristic (ROC) curve, calibration curves, and decision curve analysis.

Results: Relative to the non-pCR cohort, the pCR group exhibited smaller tumor diameters, lower Ki-67 expression, fewer lymph node metastases, and higher proportions of HER2+ molecular subtype (P<0.05). Pretreatment SUV_{max}, MTV, and TLG levels in the pCR group were significantly lower than those in the non-pCR group, and showed a marked decrease after treatment (P<0.05), whereas no significant changes were observed in the non-pCR group (P>0.05). SUV_{max}, MTV, TLG, and molecular subtype were identified as independent predictors of non-pCR through logistic regression analysis. A nomogram constructed using these predictors achieved area under the ROC curve (AUC) of 0.9003 and 0.9363 in the training and validation cohorts, respectively. The model demonstrated good calibration (Hosmer-Lemeshow test, χ^2=6.412, P=0.60) and clinical utility through decision curve analysis, effectively stratifying patients at high risk of non-pCR based on a cutoff value of 0.8230.

Conclusions: ^{18}F-FDG PET/CT demonstrates significant clinical value in predicting pCR to NACT in BC patients. By integrating metabolic parameters such as SUV_{max}, MTV, and TLG into a nomogram, this approach enables accurate prediction of treatment efficacy, aiding in the early identification of patients unlikely to benefit from NACT. This facilitates timely adjustments to personalized treatment plans, optimizing clinical outcomes and resource allocation.

Keywords: ^{18}F-fluorodeoxyglucose positron emission tomography/computed tomography (^{18}F-FDG PET/CT); neoadjuvant chemotherapy (NACT); breast cancer (BC); pathological complete response (pCR); prediction model

Submitted Dec 27, 2024. Accepted for publication Jan 15, 2025. Published online Jan 20, 2025.
doi: 10.21037/gs-2024-568
View this article at: https://dx.doi.org/10.21037/gs-2024-568

Introduction

Breast cancer (BC) is the most prevalent disease in the world and the largest contributor to cancer-associated mortality among women. The annual growth in incidence has considerably increased the global cancer burden (1). Between 2010 and 2019, the yearly incidence of BC rose by 0.5% (2). In 2020, there were more than 2.3 million newly diagnosed cases of BC and around 685,000 associated fatalities. By 2040, it is projected that more than 3 million new cases of BC will be diagnosed each year (3).

Recently, neoadjuvant chemotherapy (NACT) has been employed as the gold standard approach for managing early high-risk and locally advanced patients with BC. It can convert locally advanced and inoperable breast tumors into operable ones, slightly increase the rate of breast conservation (4,5), and reduces tumor staging and metastatic rates, extending patient survival. However, not all patients benefit from NACT due to tumor heterogeneity and complexity. In cases of patients who do not respond to treatment, although disease progression during NACT is rare, long-term treatment may cause adverse effects. This could lead to missed opportunities to alter the treatment plan (6). Therefore, a method for the early prediction of neoadjuvant therapy efficacy is urgently needed to avoid ineffective treatments and delays in surgery.

Imaging is essential in BC screening, diagnosis, staging, and management. Among the various modalities, ^{18}F-fluorodeoxyglucose (FDG) positron emission tomography/computed tomography (PET/CT) is a sensitive molecular imaging system frequently employed for cancer diagnosis, early identification of distant metastases, assessment of treatment responses in locally advanced and metastatic cancers, and prognostic risk stratification (7,8).

PET/CT parameters, such as maximum standardized uptake value (SUV_{max}), metabolic tumor volume (MTV), and total lesion glycolysis (TLG), reflect tumor glucose metabolism and total metabolic burden, providing insights into tumor heterogeneity and activity that cannot be captured by conventional imaging techniques (9-11). These parameters are particularly effective in monitoring early metabolic changes in response to NACT, which often precede morphological changes in tumor size. Thus, ^{18}F-FDG PET/CT has the potential to serve as a robust tool for predicting pathological complete response (pCR). Despite this potential, existing prediction models for pCR in BC often rely on clinical and pathological factors, with limited integration of advanced imaging parameters (12). Studies incorporating PET/CT-based models remain relatively scarce, and the predictive power of SUV_{max}, MTV, and TLG has not been fully validated in diverse clinical settings (13,14). Addressing this gap is critical for developing reliable tools that can guide personalized treatment strategies and improve outcomes for BC patients.

We conducted this study to examine the capacity of ^{18}F-FDG PET/CT to predict the efficacy of neoadjuvant chemotherapeutic among patients with BC in order to garner critical theoretical support for personalized treatment and avoid inefficient chemotherapy. We present this article in accordance with the TRIPOD reporting checklist (available at https://gs.amegroups.com/article/

Highlight box

Key findings

- In this study, parameters derived from ^{18}F-fluorodeoxyglucose (FDG) positron emission tomography-computed tomography (PET/CT), including total lesion glycolysis (TLG), metabolic tumor volume (MTV), and maximum standardized uptake value (SUV_{max}), were found to be predictive of pathological complete response (pCR) following neoadjuvant chemotherapy (NACT) in patients with breast cancer (BC). These parameters were significantly different between patients achieving pCR and those who did not.

What is known and what is new?

- ^{18}F-FDG PET/CT is widely used for cancer diagnosis, treatment response assessment, and prognostic risk stratification.
- This study specifically evaluated the predictive value of ^{18}F-FDG PET/CT parameters in predicting pCR in patients with BC after NACT, providing new insights into their role in treatment monitoring.

What is the implication, and what should change now?

- The findings suggest that ^{18}F-FDG PET/CT could serve as an effective tool in predicting treatment response in patients with BC, potentially guiding clinical decisions. Clinicians should consider incorporating these imaging biomarkers into the evaluation process to tailor treatment strategies and improve patient outcomes.

view/10.21037/gs-2024-568/rc).

Methods

General information

This study was designed as a retrospective cohort study, conducted at the Affiliated Hospital of Nantong University. A total of 95 female patients with BC who received NACT and radical surgery between December 2021 and December 2023 were included. Data were retrospectively collected from electronic medical records, including clinical characteristics, pathological findings, and imaging results from ^{18}F-FDG PET/CT scans performed before and after treatment. The efficacy of NACT was evaluated using postoperative pathological outcomes, with patients being categorized into two groups: pCR (n=46) and non-pCR (n=49). The inclusion criteria were as follows: (I) diagnosis of BC confirmed by biopsy before NACT; (II) age between 18 and 70 years; (III) a postoperative follow-up time longer than 3 months; (IV) provision of informed consent; and (V) complete clinical and pathological information. Meanwhile, the exclusion criteria were as follows: (I) bilateral BC; (II) BC concurrent with other breast diseases; (III) BC concurrent with systemic malignancies; (IV) contraindications to surgery or radiation therapy; (V) death during follow-up due to other causes; and (VI) an inability to complete required examinations and treatments. The study was conducted in accordance with the Declaration of Helsinki (as revised in 2013). The study was approved by the Affiliated Hospital of Nantong University (No. 2025-K006-01) and informed consent was taken from all the patients.

^{18}F-FDG PET/CT examination

Each participant received PET/CT scans before and following therapy. Before the scan, patients were restricted from consuming water for >6 hours, and blood glucose concentrations were maintained between 3.9 and 6.1 mmol/L on the day of the scan. ^{18}F-FDG was synthesized with the mini-trace synthesis method at a PET/CT facility, achieving a radiochemical purity of over 90%. The injection dose was calculated at 3.7 MBq/kg, and patients were advised to empty their bladder before imaging and rested in a supine position for 60 minutes post-injection. The PET/CT scanner was a 16-slice model with CT parameters set to a tube voltage of 140 kV, a tube current of 200 mA, a slice thickness of 3.27 mm, and a pitch of 1.0. PET scanning was conducted for 3 minutes per bed, with an axial field of view of 180 mm and a slice thickness of 3.27 mm. Each patient underwent 9–10 bed positions, with adjacent positions overlapping by 50%. After scanning, three-dimensional reconstruction was performed using the maximum likelihood algorithm, which was combined with CT data for attenuation correction, and images were fused using an iterative method. Two experienced nuclear medicine physicians, each with >5 years of experience, independently processed the images and delineated regions of interest (ROIs) on the largest diameter plane of abnormal metabolic areas. A manual contouring method was used for ROI delineation, ensuring accuracy by referring to the tumor's anatomical structure on CT and its metabolic activity on PET. The following PET/CT parameters were calculated: (I) SUV_{max}: SUV_{max} represents the highest uptake value of ^{18}F-FDG within the ROI and reflects the most metabolically active portion of the lesion. It is calculated as the ratio of tissue radioactivity concentration (measured by PET) to the injected dose per body weight. (II) MTV: MTV was calculated by summing the voxel volumes within the ROI that exhibited standardized uptake values (SUVs) exceeding 40% of the SUV_{max}, using the fixed % SUV_{max} threshold method (FSTM) (15). This threshold ensured that only metabolically active tumor regions were included in the calculation. MTV represents the metabolically active tumor burden. (III) TLG: TLG was computed as the product of MTV and the mean SUV within the delineated ROI. It reflects the overall glycolytic activity of the lesion and combines metabolic intensity with tumor volume.

Treatment methods

Patients received different NACT regimens based on tumor stage and type: 25 received cyclophosphamide + epirubicin + fluorouracil, and 70 received paclitaxel + epirubicin + cyclophosphamide. All patients underwent four cycles of chemotherapy. Patients received surgical treatment at our facility approximately 2 weeks following the conclusion of NACT. pCR was defined as the absence of invasive BC cells both in the primary breast tumor site and in the regional lymph nodes, whereas non-pCR was defined as the presence of invasive cancer cells in either the primary tumor site or the regional lymph nodes after treatment.

Collection of clinical and pathological information

Clinical and pathological information was obtained from

the hospital information management program and included patient age, menstrual status, clinical stage, lymph node metastasis, vascular invasion, pathological type, nerve invasion, tumor diameter, tumor location, number of lesions, Ki-67 expression status (≥14% indicating high proliferative activity and <14% indicating low proliferative activity), and molecular subtype.

Observational indicators

(I) The clinical and pathological features were assessed between the two cohorts before treatment. (II) A comparison of SUV_{max}, MTV, and TLG levels before and after therapy between the two groups was conducted. (III) Receiver operating characteristic (ROC) curve analysis was used to examine the value of the SUV_{max}, MTV, and TLG in predicting pCR following therapy. (IV) Multivariate logistic regression was used to identify the independent risk factors influencing efficacy. (V) A nomogram for non-pCR prediction was generated based on the independent risk factors associated with efficacy and on calibration curves.

Statistical analysis

GraphPad Prism 6.0 (GraphPad Software, San Diego, CA, USA) was used for creating graphs, while SPSS 26.0 (IBM Corp., Armonk, NY, USA) was employed for statistical analysis. Independent *t*-tests were used to compare groups with continuously and normally distributed data, with the results presented as the mean ± standard deviation (SD). The Mann-Whitney test was applied to data with a nonnormal distribution, which are reported as the median and interquartile range. The χ^2 test was used to compare categorical information, which are expressed the as frequency and percentage. To evaluate the predictive value of SUV_{max}, MTV, and TLG for pCR, ROC curves were plotted. The area under the ROC curve (AUC) values of 0.7–0.8 were considered acceptable, 0.8–0.9 were considered good, and >0.9 were considered excellent for prediction performance. The efficacy of NACT was determined by multivariate logistic regression analysis, and the "rms" package in R (The R Foundation for Statistical Computing) was used to create a nomogram prediction model and calibration curves for non-pCR. All P-values were two-sided, with P<0.05 set as the significance threshold.

Results

Comparison of pretreatment clinical and pathological features in pCR and non-pCR groups

Relative to the non-pCR group, the pCR group had a substantially greater portion of patients with clinical stage I–II, tumor diameter ≤3 cm, and Ki-67 expression rate ≤14% and a lower portion of lymph node metastases (P<0.05). The molecular subtype pattern revealed a marked difference between the two cohorts (P<0.05). The HR+HER2+ (Hormone Receptor Positive and Human Epidermal Growth Factor Receptor 2 Positive) subtype was most prevalent in the pCR group, whereas the HR+HER2– (HR positive and HER2 negative) subtype was more frequent in the non-pCR group. No significant differences were observed in the other clinical and pathological features (P>0.05; *Table 1*).

Changes in SUV_{max}, MTV, and TLG levels before and after treatment

The TLG, MTV, and SUV_{max} levels in the pCR group were considerably lower than those in the non-pCR group

Table 1 Detailed clinical and pathological characteristics before treatment in the pCR and non-pCR groups

Clinical data	pCR (n=46)	Non-pCR (n=49)	*t*	P
Age (years)			0.002335	0.96
≤50	27 (58.70)	29 (59.18)		
>50	19 (41.30)	20 (40.82)		
Menstrual status			0.7688	0.38
Premenopausal	31 (67.39)	37 (75.51)		
Postmenopausal	15 (32.61)	12 (24.49)		

Table 1 *(continued)*

Table 1 *(continued)*

Clinical data	pCR (n=46)	Non-pCR (n=49)	*t*	P
TNM staging			4.6333	0.03
Stage I–II	28 (60.87)	19 (38.78)		
Stage III–IV	18 (39.13)	30 (61.22)		
Lymph node metastasis			4.6333	0.03
No	28 (60.87)	19 (38.78)		
Yes	18 (39.13)	30 (61.22)		
Vascular invasion			1.6498	0.20
No	33 (71.74)	29 (59.18)		
Yes	13 (28.26)	20 (40.82)		
Pathological type			1.277	0.53
Invasive ductal carcinoma	39 (84.78)	37 (75.51)		
Invasive lobular carcinoma	4 (8.70)	7 (14.29)		
Other	3 (6.52)	5 (10.20)		
Nerve invasion			0.9699	0.32
No	29 (63.04)	26 (53.06)		
Yes	17 (36.96)	23 (46.94)		
Tumor diameter (cm)			5.5337	0.02
≤3	28 (60.87)	18 (36.73)		
>3	18 (39.13)	31 (63.27)		
Tumor location			0.2262	0.63
Outer quadrant	25 (54.35)	29 (59.18)		
Central or inner quadrant	21 (45.65)	20 (40.82)		
Number of lesions			1.6235	0.20
1	5 (10.87)	10 (20.41)		
>1	41 (89.13)	39 (79.59)		
Ki-67			18.99	<0.001
≤14%	38 (82.61)	19 (38.78)		
>14%	8 (17.39)	30 (61.22)		
Molecular subtype			18.52	<0.001
HR+HER2−	6 (13.04)	27 (55.10)		
TNBC	11 (23.91)	6 (12.24)		
HR+HER2+	15 (32.61)	8 (16.33)		
HR−HER2+	14 (30.44)	8 (16.33)		

Data are presented as n (%). pCR, pathological complete response; TNM, tumor, node, metastasis; HR, hormone receptor; HER2, human epidermal growth factor receptor 2; TNBC, triple-negative breast cancer.

Table 2 Variations in SUV_{max}, MTV, and TLG metrics pre- and posttreatment in the pCR and non-pCR groups

Group	SUV_{max}	MTV (cm^3)	TLG (g)
pCR			
Pretreatment	11.29 (6.38, 11.63)	32.70±10.33	259.00 (205.94, 288.92)
Posttreatment	6.00 (3.94, 8.05)	13.96±3.61	54.24 (46.41, 59.97)
t/*Z*	−4.377	11.61	−7.993
P	<0.001	<0.001	<0.001
Non-pCR			
Pretreatment	13.21 (11.87, 14.18)****	43.01±14.68***	259.90 (239.35, 354.60)**
Posttreatment	12.44 (11.38, 13.67)****	40.31±7.66****	255.67 (228.11, 339.56)****
t/*Z*	−1.5987	1.1426	−1.3926
P	0.11	0.26	0.17

Data are presented as x±SD or M (P25, P75). Compared with pretreatment and posttreatment in the pCR group: **, P<0.01; ***, P<0.001; ****, P<0.0001. SUV_{max}, maximum standardized uptake value; MTV, metabolic tumor volume; TLG, total lesion glycolysis; pCR, pathological complete response; SD, standard deviation.

Table 3 Predictive value of SUV_{max}, MTV, and TLG for pCR

Indicator	AUC	SE	P value	95% CI	Sensitivity (%)	Specificity (%)	Cutoff value	Youden index
Pretreatment SUV_{max}	0.7753	0.05056	<0.001	0.6762–0.8744	82.61	73.47	12.18	0.5608
Pretreatment MTV (cm^3)	0.7010	0.05380	<0.001	0.5955–0.8064	91.30	48.98	44.88	0.4028
Pretreatment TLG (g)	0.6624	0.05611	0.006	0.5524–0.7724	39.13	91.84	224.44	0.3097

SUV_{max}, maximum standardized uptake value; MTV, metabolic tumor volume; TLG, total lesion glycolysis; pCR, pathological complete response; AUC, area under curve.

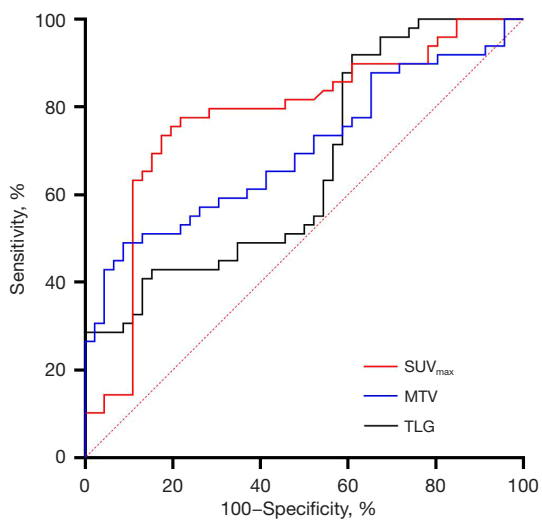

Figure 1 Analysis of predictive efficacy. SUV_{max}, maximum standardized uptake value; MTV, metabolic tumor volume; TLG, total lesion glycolysis.

both before and after treatment (P<0.05). Moreover, the pCR group exhibited substantially lower SUV_{max}, MTV, and TLG levels after treatment relative to pretreatment measurements. Conversely, the non-pCR group showed no significant difference in SUV_{max}, MTV, or TLG levels from before to after treatment (P>0.05; *Table 2*).

ROC curves of SUV_{max}, MTV, and TLG and the prediction of pCR

According to ROC curve analysis, the AUCs for predicting the neoadjuvant chemotherapeutic efficacy among the patients with BC before treatment were 0.7753 for SUV_{max}, 0.7010 for MTV, and 0.6624 for TLG; the sensitivities were 82.61%, 91.30%, and 39.13%, respectively, while the specificities were 73.47%, 48.98%, and 91.84%, respectively (P<0.05). These findings indicated good clinical predictive value (*Table 3* and *Figure 1*).

Table 4 Multivariate analysis of variables influencing treatment efficacy

Influencing factors	P	Exp(B)	95% CI
TNM staging	0.19	3.6726	0.5153–26.1756
Lymph node metastasis	0.12	5.2926	0.6429–43.5692
Tumor diameter	0.93	1.0869	0.1594–7.4092
Ki-67	0.10	3.8763	0.7624–19.7076
Molecular type (HR+HER2–)			
TNBC	0.002	0.0098	0.0005–0.1868
HR+HER2+	0.009	0.0522	0.0057–0.4751
HR–HER2+	0.003	0.0106	0.0006–0.2032
Pretreatment SUV_{max}	0.02	1.2685	1.0456–1.5389
Pretreatment MTV	0.004	1.1325	1.0418–1.2311
Pretreatment TLG	0.02	1.0181	1.0031–1.0333

TNM, tumor, node, and metastasis; HR, hormone receptor; HER2, human epidermal growth factor receptor 2; TNBC, triple-negative breast cancer; SUV_{max}, maximum standardized uptake value; MTV, metabolic tumor volume; TLG, total lesion glycolysis; CI, confidence interval.

A nomogram model for predicting non-pCR in patients treated with NACT for BC

Analysis of independent risk factors influencing efficacy

Factors with statistically significant differences were included as independent variables, with non-pCR after NACT as the dependent variable (no =0, yes =1). Multivariate logistic regression analysis revealed that molecular subtype and pretreatment SUV_{max}, MTV, and TLG levels were independent risk factors associated with treatment efficacy (*Table 4*).

Development of the nomogram model

To conduct our multivariate analysis, we randomly separated 95 study participants into a training and validation cohort in a 7:3 ratio using the "rms" R package. Subsequently, a nomogram prediction model was created to predict the possibility that patients with BC would not achieve a positive response after NACT (*Figure 2A*).

In the nomogram presented in *Figure 2A*, for the "Molecular subtype" axis, "0" represents the HR+HER2– subtype, "1" represents the triple-negative BC (TNBC) subtype, "2" represents the HR+HER2+ subtype, and "3" represents the HR–HER2+ subtype. The "Pretreatment SUV_{max}" axis represents the SUV_{max} level before NACT. The "Pretreatment MTV" axis represents the MTV level before NACT. The "Pretreatment TLG" axis represents the TLG level before NACT. The "Risk" axis indicates the model's prediction of the risk of non-pCR. The ROC curve for this nomogram model is shown in *Figure 2B*. According to the findings, the training cohort's AUC was 0.9003 [95% confidence interval (CI): 0.8278–0.9728], and its sensitivity and specificity were 0.9655 (95% CI: 0.8991–1.0000) and 0.7027 (95% CI: 0.5554–0.8500), respectively. An AUC of 0.9363 (95% CI: 0.8542–1.0000), along with a sensitivity of 0.9412 (95% CI: 0.8293–1.0000) and a specificity of 0.6667 (95% CI: 0.3999–0.9334), indicating good accuracy, were obtained from bootstrap analyses used for internal validation of the nomogram (*Table 5*).

The cutoff value for this model was 0.8230. In this study, a risk score ≥0.8230 was considered to indicate high risk for non-pCR following NACT, while a score <0.8230 indicated low risk.

An example application of the nomogram is described below (*Figure 2A*): for a patient with BC with an HR+HER2– molecular subtype, a pre-treatment SUV_{max} level of 15.00, an MTV level of 25.00, and a TLG level of 175.00, the corresponding to "Points" values for the molecular subtype, pre-treatment SUV_{max}, pre-treatment MTV, and pre-treatment TLG are 63, 37.5, 28.5, and 23, respectively. The sum of these values gives a total score of 152. Based on the "Total Points" scale, this score represents a risk value of approximately 0.7 on the "Risk" axis. Since 0.7<0.8230, the model predicts that this patient has a low risk of non-pCR following NACT.

Calibration curve and decision curve analysis

The Hosmer-Lemeshow (HL) test is an indicator of model fit. A P value >0.05 indicates the model fits rather well, implying no appreciable variation between expected and actual values. The HL test findings for this model were a χ^2 value of 6.412 and a P value of 0.6012, suggesting an adequate model fit. Furthermore, the calibration curve indicated that the expected and actual probabilities were generally consistent (*Figure 3A*).

Clinical decision curve analysis is a relatively new method for evaluating the clinical effectiveness of predictive models. The clinical decision curve for the non-pCR risk nomogram showed that compared to the scenarios in which all patients were classified as non-pCR (red diagonal line in *Figure 3B*) or all as pCR (green horizontal line in *Figure 3B*), the nomogram model provided an excellent net clinical benefit in the threshold range of 0.05 to 1 (*Figure 3B*).

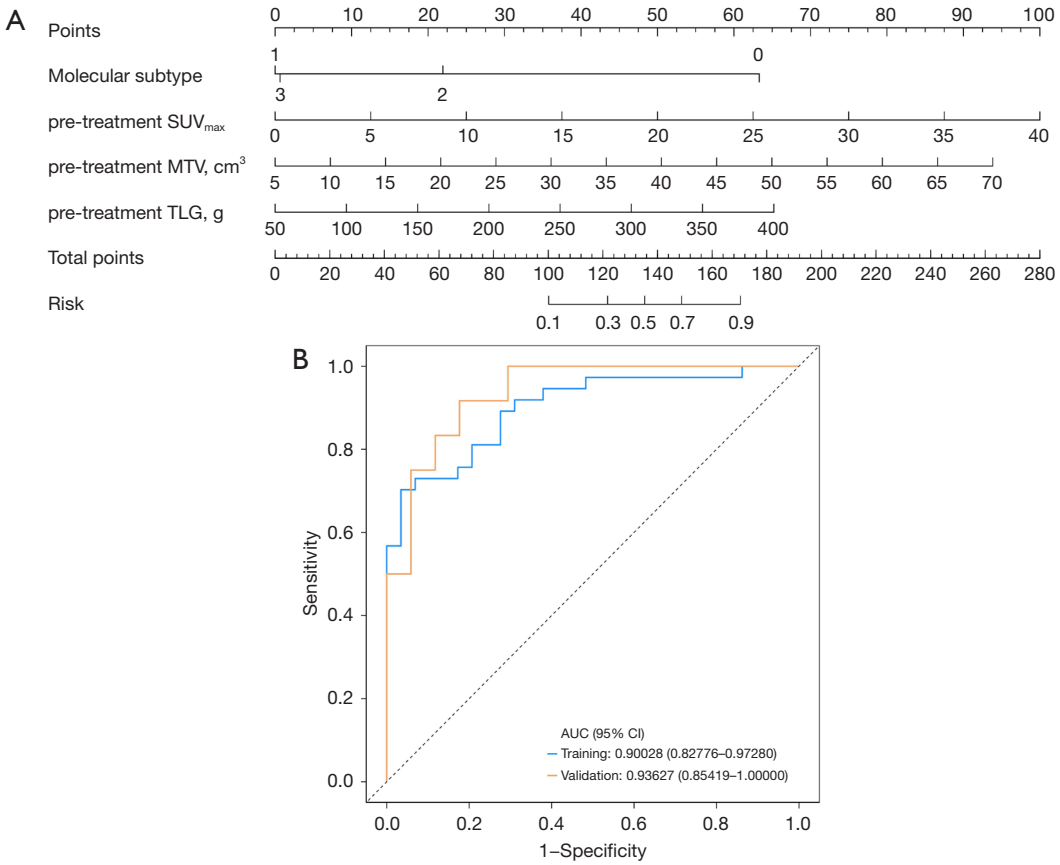

Figure 2 Predictive tools for breast cancer treatment outcomes. (A) Nomogram for predicting non-pCR in patients undergoing neoadjuvant chemotherapy for breast cancer. (B) Validation of the nomogram using ROC curve analysis. SUV_{max}, maximum standardized uptake value; MTV, metabolic tumor volume; TLG, total lesion glycolysis; AUC, area under the ROC curve; CI, confidence interval; pCR, pathological complete response; ROC, receiver operating characteristic.

Table 5 ROC curve data for the training and validation sets

Data	AUC (95% CI)	Sensitivity (95% CI)	Specificity (95% CI)	Cutoff
Training	0.9003 (0.8278–0.9728)	0.9655 (0.8991–1.0000)	0.7027 (0.5554–0.8500)	0.8230
Test	0.9363 (0.8542–1.0000)	0.9412 (0.8293–1.0000)	0.6667 (0.3999–0.9334)	0.8230

ROC, receiver operating characteristic; AUC, area under the ROC curve; CI, confidence interval.

Discussion

NACT is used extensively as an all-encompassing treatment of BC. However, only about 20% of patients receiving NACT can obtain pCR. Patients exhibiting extended disease-free survival and overall survival (OS) contrast with those without pCR patients, who may encounter disease progression and unfavorable prognosis (16). Therefore, predicting the efficacy of NACT in BC is essential for targeted therapy. Compared to conventional imaging techniques, ^{18}F-FDG PET/CT can detect tumor response at an earlier stage, demonstrating the significant potential for predicting the efficacy of NACT (17-19). Tumor metabolic changes occur before a reduction in tumor size, and FDG uptake reflects tumor metabolic activity (20,21). According to Abdelrahman *et al.* (22), ^{18}F-FDG PET/CT can reliably predict, at an early stage, the pathological response of locally progressed or borderline resectable pancreatic cancer

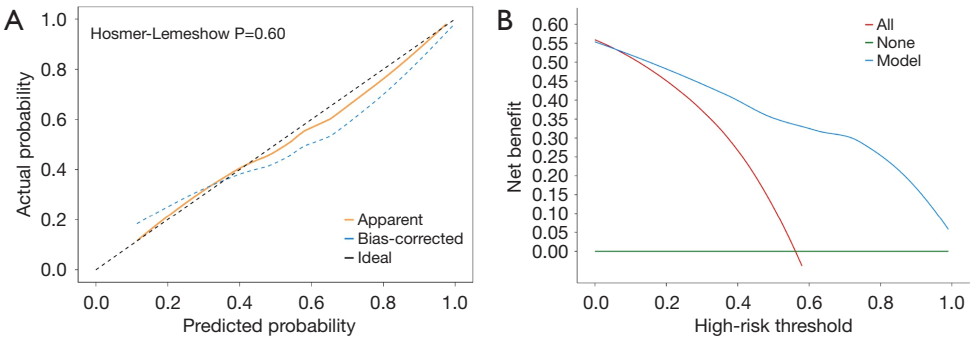

Figure 3 Assessment of the non-pCR risk prediction model in neoadjuvant chemotherapy. (A) Calibration curve for the model. (B) DCA curve for evaluating the clinical utility of the model in predicting non-pCR. pCR, pathological complete response; DCA, decision curve analysis.

to NACT. Mi *et al.* (23) provided evidence that a significant decrease in TLG, MTV, and SUV_{max} of the primary tumor is linked to improved OS and progression-free survival, indicating that ^{18}F-FDG PET/CT can accurately reflect chemotherapy efficacy before and after NACT. In the study by Sengoz *et al.* (24), the only independent predictor of pCR was ΔSUV_{max}, with responders having a ΔSUV_{max} much greater than that of nonresponders. This suggests that ^{18}F-FDG PET/CT is a valuable tool for assessing treatment outcomes following NACT for BC. Our analysis indicated that before treatment, SUV_{max}, MTV, and TLG levels were considerably elevated among the non-pCR group relative to the pCR group, which is consistent with above study. Following treatment, the pCR group's SUV_{max}, MTV, and TLG levels substantially decreased, but those of the non-pCR group showed no change. This implies that ^{18}F-FDG PET/CT features are potentially robust predictors of neoadjuvant therapeutic efficacy.

Additionally, the comparison of clinical and pathological features revealed marked differences between the two cohorts in clinical stage, tumor diameter, Ki-67 expression rate, lymph node metastasis, and molecular subtype. This can be explained by the strong association between ^{18}F-FDG PET/CT parameters and tumor progression. Elevated TLG, MTV, and SUV_{max} levels suggest increased tumor burden and active metabolism (25). Higher clinical stages (26), larger tumor diameters (27), lymph node metastasis (28), and increased Ki-67 expression (29) are all clinical indicators of tumor progression, reflecting greater tumor invasiveness and increased metabolic activity. This can explain the significant higher ^{18}F-FDG PET/CT values in the non-pCR group than in the pCR group in this study. Moreover, the heterogeneity in BC subtypes, such as invasive lobular carcinoma and invasive ductal carcinoma, has been reported to contribute to differences in metabolic activity and response rates to NACT (30). For example, invasive ductal carcinoma, which is the most common subtype, tends to demonstrate higher metabolic activity on ^{18}F-FDG PET/CT compared to invasive lobular carcinoma, which often exhibits lower FDG uptake due to its histological characteristics (31,32). However, in our study, the distribution of pathological subtypes between the pCR and non-pCR groups showed no significant differences. These findings suggest that the observed differences in MTV, TLG, and SUV_{max} levels between the two groups may not be directly attributed to the distribution of pathological subtypes in this cohort. Instead, other factors, such as molecular subtypes and tumor metabolic burden, likely play a more prominent role in influencing the metabolic parameters. Furthermore, variations in molecular subtypes also play a significant role in the response to NACT. For instance, NACT provides a higher pCR rate in HER2+ patients (33). In a study on high-risk early BC, the estimated pCR prevalence for the HER2+ group was much higher than that of the HER2 group (74% *vs.* 30%) (34). Similarly, our study observed that the pCR group had the highest proportion of HER2+ patients. These findings suggest that the differences in MTV, TLG, and SUV_{max} levels may primarily reflect the tumor's metabolic burden and molecular characteristics.

Our study employed pretreatment ^{18}F-FDG PET-CT parameters to estimate the neoadjuvant chemotherapeutic efficacy, thereby enhancing the predictive power of ^{18}F-FDG PET-CT in this regard. Although the validity of each parameter differs, ROC curve analysis demonstrated that each represents a robust means to evaluating neoadjuvant chemotherapeutic efficacy in patients with

BC. Among the parameters, SUV_{max} had the highest AUC, MTV had the highest sensitivity, and TLG had the highest specificity. Thus, combining all three parameters may provide a comprehensive assessment of chemotherapy efficacy, aiding clinicians in the timely adjustment of treatment plans during neoadjuvant therapy.

Studies on the variables influencing the neoadjuvant chemotherapeutic efficacy in BC are currently scarce. Existing studies report different independent factors due to variations in study populations and clinical data. Jiao *et al.* (35) observed that in patients with initial ipsilateral supraclavicular lymph node metastases, the degree of Ki-67 expression was an independent risk factor influencing pCR. Our study found that molecular subtype and TLG, MTV, and SUV_{max} pretreatment levels were independent risk factors influencing NACT efficacy. Higher levels of TLG, MTV, and SUV_{max} before treatment and a molecular subtype of HR+HER2– were associated with a higher risk of non-pCR. Based on genetic subtype and pr-treatment TLG, MTV, and SUV_{max}, we constructed a nomogram prediction model for non-pCR with strong predictive power and practical value. The model's repeatability and dependability were confirmed using the HL test and calibration curves, which demonstrated a close relationship between expected and actual risks. In clinical practice, this model can be used to evaluate the actual efficacy of NACT, identify non-responders early, and adjust treatment plans promptly to improve patient outcomes and survival rates. Decision curve analysis assesses the decision utility of the model, with net benefit defined as the difference between the expected benefit and harm of each prediction model (36). The decision curve analysis results of this study indicated the significant predictive capability of the clinical prediction model. This study, while having produced promising results, was retrospective in nature, included a limited sample sized, and recruited participants from a single center, which represent its inherent limitations. Additional research with a larger sample size and a multicenter design is essential to enhancing the precision of ^{18}F-FDG PET/CT in predicting the efficacy of NACT and to better inform clinical treatment decision-making.

Conclusions

The ^{18}F-FDG PET/CT measures of TLG, MTV, and SUV_{max} possess significant clinical utility in the early prediction of pCR following NACT. They can accurately assess the efficacy of NACT, thereby helping to avoid ineffective treatment and providing a basis for personalized treatment plans.

Acknowledgments

None.

Footnote

Reporting Checklist: The authors have completed the TRIPOD reporting checklist. Available at https://gs.amegroups.com/article/view/10.21037/gs-2024-568/rc

Data Sharing Statement: Available at https://gs.amegroups.com/article/view/10.21037/gs-2024-568/dss

Peer Review File: Available at https://gs.amegroups.com/article/view/10.21037/gs-2024-568/prf

Funding: This study was supported by the Nantong Science and Technology Project (2022 Social and Livelihood - General Project - Public Health) (No. MS22022044).

Conflicts of Interest: All authors have completed the ICMJE uniform disclosure form (available at https://gs.amegroups.com/article/view/10.21037/gs-2024-568/coif). The authors have no conflicts of interest to declare.

Ethical Statement: The authors are accountable for all aspects of the work in ensuring that questions related to the accuracy or integrity of any part of the work are appropriately investigated and resolved. The study was conducted in accordance with the Declaration of Helsinki (as revised in 2013). The study was approved by the Affiliated Hospital of Nantong University (No. 2025-K006-01) and informed consent was taken from all the patients.

References

1. Katsura C, Ogunmwonyi I, Kankam HK, et al. Breast cancer: presentation, investigation and management. Br J Hosp Med (Lond) 2022;83:1-7.
2. Huang X, Song C, Zhang J, et al. Circular RNAs in breast cancer diagnosis, treatment and prognosis. Oncol Res 2023;32:241-9.
3. Sung H, Ferlay J, Siegel RL, et al. Global Cancer Statistics 2020: GLOBOCAN Estimates of Incidence and Mortality Worldwide for 36 Cancers in 185 Countries. CA Cancer J Clin 2021;71:209-49.
4. Aebi S, Karlsson P, Wapnir IL. Locally advanced breast cancer. Breast 2022;62 Suppl 1:S58-62.
5. Montagna G, Mrdutt MM, Sun SX, et al. Omission of Axillary Dissection Following Nodal Downstaging With Neoadjuvant Chemotherapy. JAMA Oncol 2024;10:793-8.
6. Zaborowski AM, Wong SM. Neoadjuvant systemic therapy for breast cancer. Br J Surg 2023;110:765-72.
7. Fowler AM, Strigel RM. Clinical advances in PET-MRI for breast cancer. Lancet Oncol 2022;23:e32-43.
8. Chen F, Jiang J, Peng Y, et al. A machine learning model incorporating 18F-prostate-specific membrane antigen-1007 positron emission tomography/computed tomography and multiparametric magnetic resonance imaging for predicting prostate-specific antigen persistence in patients with prostate cancer after radical prostatectomy. Quant Imaging Med Surg 2025;15:30-41.
9. Gui X, Liang X, Guo X, et al. Impact of HER2-targeted PET/CT imaging in patients with breast cancer and therapeutic response monitoring. Oncologist 2024;oyae188.
10. Seban RD, Arnaud E, Loirat D, et al. 18FFDG PET/CT for predicting triple-negative breast cancer outcomes after neoadjuvant chemotherapy with or without pembrolizumab. Eur J Nucl Med Mol Imaging 2023;50:4024-35.
11. Arslan E, Can Trabulus D, Mermut Ö, et al. Alternative volumetric PET pjmirometers for evaluation of breast cancer cases with 18F-FDG PET/CT imaging: Metabolic tumour volume and total lesion glycolysis. J Med Imaging Radiat Oncol 2021;65:38-45.
12. van den Ende NS, Nguyen AH, Jager A, et al. Triple-Negative Breast Cancer and Predictive Markers of Response to Neoadjuvant Chemotherapy: A Systematic Review. Int J Mol Sci 2023;24:2969.
13. Wu Y, Li Y, Chen B, et al. 18F-FDG PET/CT for early prediction of pathological complete response in breast cancer neoadjuvant therapy: a retrospective analysis. Oncologist 2024;29:e1646-55.
14. Zheng X, Huang Y, Lin Y, et al. (18)F-FDG PET/CT-based deep learning radiomics predicts 5-years disease-free survival after failure to achieve pathologic complete response to neoadjuvant chemotherapy in breast cancer. EJNMMI Res 2023;13:105.
15. Zhang Y, Hu Y, Zhao S, et al. The Utility of PET/CT Metabolic Parameters Measured Based on Fixed Percentage Threshold of SUVmax and Adaptive Iterative Algorithm in the New Revised FIGO Staging System for Stage III Cervical Cancer. Front Med (Lausanne) 2021;8:680072.
16. Zhang J, Wu Q, Yin W, et al. Development and validation of a radiopathomic model for predicting pathologic complete response to neoadjuvant chemotherapy in breast cancer patients. BMC Cancer 2023;23:431.
17. Liu D, Lin D, Lin Z, et al. Development and validation of a nomogram for incorporating (18)F-FDG PET/CT spleen uptake for predicting prognosis in elderly esophageal cancer patients treated with radiotherapy. J Thorac Dis 2024;16:7853-65.
18. Huang W, Xiong Z, Zhong W, et al. Development of a nomogram for predicting survival of breast cancer patients with neoadjuvant chemotherapy: a dynamic analysis for systemic inflammation response index. Gland Surg 2023;12:1459-74.
19. He M, Su J, Ruan H, et al. Nomogram based on quantitative dynamic contrast-enhanced magnetic resonance imaging, apparent diffusion coefficient, and clinicopathological features for early prediction of pathologic complete response in breast cancer patients receiving neoadjuvant chemotherapy. Quant Imaging Med Surg 2023;13:4089-102.
20. Owens C, Hindocha S, Lee R, et al. The lung cancers: staging and response, CT, (18)F-FDG PET/CT, MRI, DWI: review and new perspectives. Br J Radiol 2023;96:20220339.
21. Groheux D. Breast Cancer Systemic Staging (Comparison of Computed Tomography, Bone Scan, and 18F-Fluorodeoxyglucose PET/Computed Tomography). PET Clin 2023;18:503-15.
22. Abdelrahman AM, Goenka AH, Alva-Ruiz R, et al. FDG-PET Predicts Neoadjuvant Therapy Response and Survival in Borderline Resectable/Locally Advanced Pancreatic Adenocarcinoma. J Natl Compr Canc Netw 2022;20:1023-1032.e3.
23. Mi L, Zhao Y, Zhao X, et al. (18)F-Fluorodeoxyglucose

Positron Emission Tomography-Computed Tomography Metabolic Parameters Before and After Neoadjuvant Chemotherapy Can Predict the Postoperative Prognosis of Locally Advanced Gastric Cancer. Cancer Biother Radiopharm 2021;36:662-71.
24. Sengoz T, Arman Karakaya Y, Gültekin A, et al. Role of F-18 FDG PET/CT in Predicting Response to Neoadjuvant Chemotherapy in Invasive Ductal Breast Cancer. Eur J Breast Health 2023;19:159-65.
25. Xu P, Wang Y. Application of (18)F-FDG PET/CT in evaluation of curative effect and prognosis for small cell lung cancer. Zhong Nan Da Xue Xue Bao Yi Xue Ban 2020;45:1255-60.
26. O'Shea AS. Clinical Staging of Ovarian Cancer. Methods Mol Biol 2022;2424:3-10.
27. Gouda MA, Janku F, Wahida A, et al. Liquid Biopsy Response Evaluation Criteria in Solid Tumors (LB-RECIST). Ann Oncol 2024;35:267-75.
28. Dieterich LC, Tacconi C, Ducoli L, et al. Lymphatic vessels in cancer. Physiol Rev 2022;102:1837-79.
29. Zhang A, Wang X, Fan C, et al. The Role of Ki67 in Evaluating Neoadjuvant Endocrine Therapy of Hormone Receptor-Positive Breast Cancer. Front Endocrinol (Lausanne) 2021;12:687244.
30. O'Connor DJ, Davey MG, Barkley LR, et al. Differences in sensitivity to neoadjuvant chemotherapy among invasive lobular and ductal carcinoma of the breast and implications on surgery-A systematic review and meta-analysis. Breast 2022;61:1-10.
31. Jung NY, Kim SH, Kim SH, et al. Effectiveness of Breast MRI and (18)F-FDG PET/CT for the Preoperative Staging of Invasive Lobular Carcinoma versus Ductal Carcinoma. J Breast Cancer 2015;18:63-72.
32. Hogan MP, Goldman DA, Dashevsky B, et al. Comparison of 18F-FDG PET/CT for Systemic Staging of Newly Diagnosed Invasive Lobular Carcinoma Versus Invasive Ductal Carcinoma. J Nucl Med 2015;56:1674-80.
33. Cantini L, Trapani D, Guidi L, et al. Neoadjuvant therapy in hormone Receptor-Positive/HER2-Negative breast cancer. Cancer Treat Rev 2024;123:102669.
34. Wolf DM, Yau C, Wulfkuhle J, et al. Redefining breast cancer subtypes to guide treatment prioritization and maximize response: Predictive biomarkers across 10 cancer therapies. Cancer Cell 2022;40:609-623.e6.
35. Jiao DC, Zhu JJ, Qiao JH, et al. The influence factors of pathologic complete response of the ipsilateral supraclavicular lymph node of breast cancer after neoadjuvant chemotherapy. Zhonghua Yi Xue Za Zhi 2019;99:2989-93.
36. Zhang W, Ji L, Wang X, et al. Nomogram Predicts Risk and Prognostic Factors for Bone Metastasis of Pancreatic Cancer: A Population-Based Analysis. Front Endocrinol (Lausanne) 2021;12:752176.

(English Language Editor: J. Gray)

Cite this article as: Ge C, Shi L, Tan Z. ^{18}F-fluorodeoxyglucose positron emission tomography-computed tomography for predicting pathological complete response to neoadjuvant chemotherapeutic in breast cancer patients. Gland Surg 2025;14(1):48-59. doi: 10.21037/gs-2024-568